Journal of Health Administration

Summer 2022, Vol 25, Issue 2

Original Article

Myocardial fibrosis delineation in Late Gadolinium Enhancement images of Hypertrophic Cardiomyopathy patients using Deep Learning methods

Mostafa Langarizadeh [1], Mahya Jahanshahi [2*], Toktam khatibi [3]

[1] *Associate Professor, School of Health Management and Information Sciences, Iran University of Medical Sciences, Tehran, Iran.*
[2] *M.Sc. Student, School of Health Management and Information Sciences, Iran University of Medical Sciences, Tehran, Iran.*
[3] *Associate Professor, School of Industrial and Systems Engineering, Tarbiat Modares University, Tehran, Iran.*

ARTICLE INFO

Corresponding Author:
Mahya Jahanshahi
e-mail addresses:
jahanshahi.m@iums.ac.ir

Received: 11/Mar/2022
Modified: 15/Jun/2022
Accepted: 20/Jun/2022
Available online: 24/Dec/2022

Keywords:
Deep Learning
Cardiac Magnetic Resonance
CMR
Myocardial Fibrosis

ABSTRACT

Introduction: Accurate delineation of myocardial fibrosis in Late Gadolinium Enhancement Cardiac Magnetic Resonance (LGE-CMR) has a crucial role in the assessment and risk stratification of HCM patients. As this is time-consuming and requires expertise, automation can be essential in accelerating this process. This study aims to use Unet-based deep learning methods to automate the mentioned process.
Methods: This study used three consecutive Unet-based networks for Region of Interest (ROI) detection, myocardial segmentation, and fibrosis delineation. The study was conducted on LGE images of 41 images diagnosed with HCM, which were contoured by two experts.
Results: This model reported a Dice similarity coefficient and accuracy of 89.74 and 98.22 in myocardial segmentation and 88.42 and 94.66 in fibrosis delineation, respectively, and could outperform the previous methods
Conclusion: The results confirm that using deep learning methods for delineating myocardial fibrosis not only can automate the process, but also helps improve the results and decrease the required time.

Extended Abstract

Introduction

Hypertrophic Cardiomyopathy (HCM) is one of the most common genetic heart muscle diseases defined by the presence of unexplained left ventricular (LV) hypertrophy. [1,2] Fibrosis is the main histologic characteristic of HCM pathology, associated with all HCM adverse outcomes such as sudden cardiac death, heart failure, and ventricular tachycardia. Therefore, fibrosis assessment is of great need for the risk analysis of HCM patients. [3] Cardiac magnetic resonance imaging (CMR) with late gadolinium enhancement (LGE) is the gold standard method for fibrosis assessment in HCM patients. [4] As a sign of fibrosis, LGE is a strong predictor of HCM complications. Hence, LGE assessment is an essential step in the proper management of HCM patients. [5,6] Segmentation of myocardial fibrosis as the first step of LGE assessment is a tedious task that needs time and expertise. [4] Thus, offering a method to automate the process can help to reduce the time and expertise needed. The previous studies worked on the automation of LGE contouring can be divided into two major groups: Image intensity-based methods such as Full Width at Half Maxim (FWHM)[7], Signal Threshold to Reference Mean (STRM)[8] and region growing [9]; or energy minimization-based methods such as graph cuts, level sets and max flow-based methods [10–14]. These methods depended on either expert user interaction such as selecting initial points, or a manual pre-segmentation of myocardial borders. In addition, most of the mentioned methods are highly sensitive to image noise. [15] With the advent of Machine Learning and Deep Learning, many studies have tried to tackle the problem using classical Machine Learning methods [16,17] or multiple deep Convolutional Neural Networks (CNN) [18–26], but none of those were able to completely automate the process of eliminating the non-ischemic fibrosis and eliminate the need of any manual pre-processing and user interaction.

This study uses a deep learning-based architecture to eliminate the need for any user interaction and fully automate the fibrosis delineation process in LGE images of HCM patients.

Methods

The architecture used in this model is composed of three consecutive SD-Unet [27] networks. Figure 1 shows a schematic view of the architecture. The first network by detecting the ROI region (Left Ventricle), reduces the class imbalance towards the background. Removing the extra parts of images in this part also helps with reducing computational complexity of the network. The second network automate the process of segmenting myocardial borders and therefore eliminates the need for manual interventions and initial pre-processing. The third network fully delineates the fibrosis borders. Dataset:This study was carried out on LGE images of 41 patients diagnosed with HCM, referred to the MRI Center at Rajaei Hospital in Tehran, Iran, between 2015 and 2018. The process of delineating the ground truth images was conducted by an experienced radiologist using segment software and revised by another if necessary. This process was done in the following three steps: In order to detect the ROI region and produce the ground truth of first network, a bounding box was drawn around the Left Ventricle in all of the images. In the second step, endocardial and epicardial borders were contoured (ground truth of second network). At the end, in order to produce the ground truth data for the third network, the fibrosis borders were fully delineated.

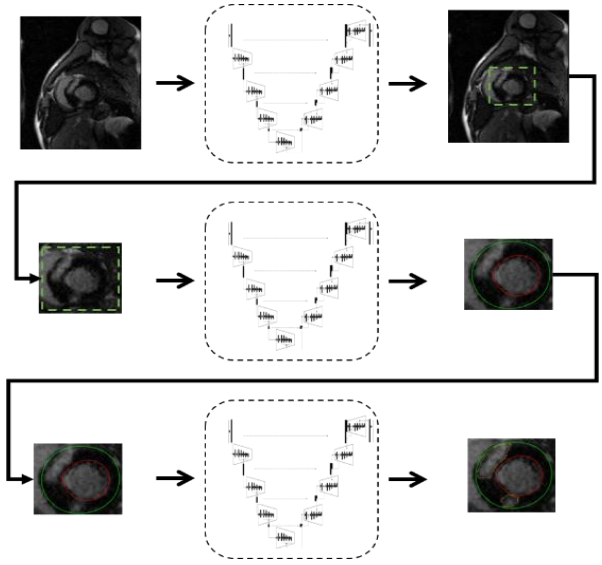

Figure 1: Schematic view of the used architecture

Network architecture: The architecture used in this paper is composed of three consecutive SD-Unet networks. SD-Unet is an encoder-decoder architecture. As displayed in Figure 2, any encoder block contains a 2*2 Maxpool layer (red arrow), followed by one 3*3 standard convolution (blue arrow) and 4 dilated convolutions (yellow arrows). At any step, the output of all these convolutions concatenates and feeds to the next layer. While increasing the dilation rate at any step, the channel numbers decrease. This leads to increasing the receptive field and therefore helps with the problem of degrading correlation between pixels while downsampling the images by the encoder. The Decoder unit upsamples the output size of the previous layer and concatenates it with the output of its corresponding layer at the encoder using skip connections (green arrows). Skip connections combine the feature maps of the encoder and decoder and provide more information about image features. In the end, one 1*1 convolution (light green arrow) is placed to convert the number of feature maps to the required number of channels and produce the contoured image.

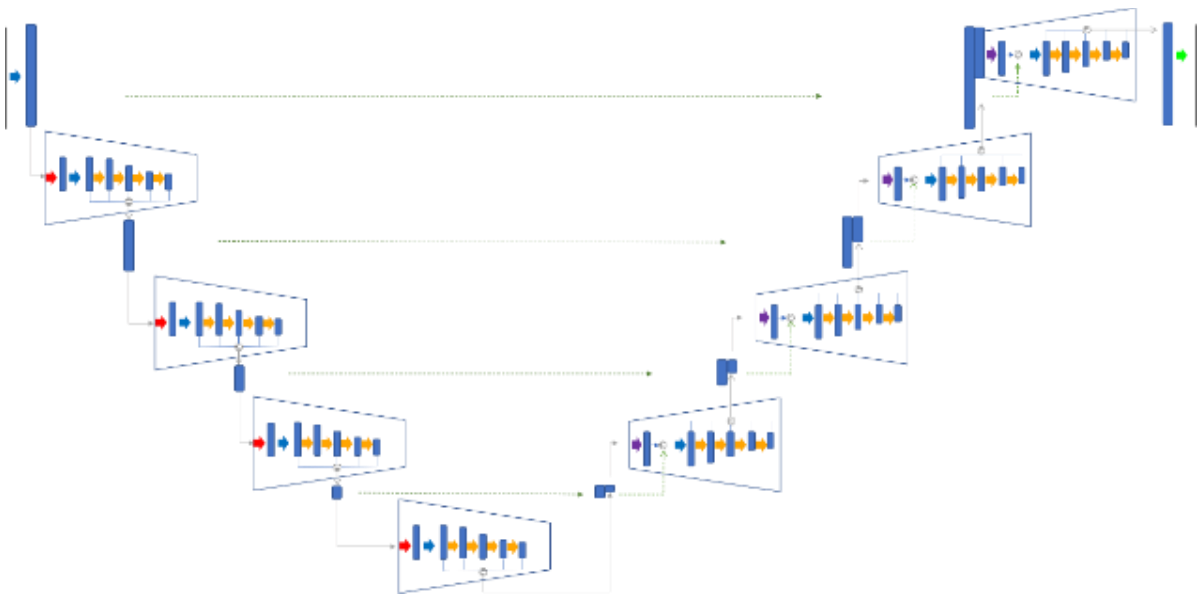

Figure 2: SD-Unet architectur

Network training and validation: The 5-fold cross-validation method was used in the division of the images as training and test data. The network was trained using the cross-entropy loss function. Adaptive moment estimation optimizer was adopted to estimate parameters and minimize the cost function.

Network Evaluation: Dice coefficient, Hausdorff distance, accuracy, precision, and recall were used to estimate the network's performance.

$$\text{Dice coefficient} = \frac{2TP}{FP + FN + 2TP} \quad \text{(Eq. 1)}$$

$$D(A,B) = \min_{a \in A} \{ \min_{b \in B} \{ d(a,b) \} \} \quad \text{(Eq. 2)}$$

$$\text{Accuracy} = \frac{TP + TN}{n} \quad \text{(Eq. 3)}$$

$$\text{Precision} = \frac{TP}{TP + FP} \quad \text{(Eq. 4)}$$

$$\text{Recall} = \frac{TP}{TP + FN} \quad \text{(Eq. 5)}$$

In the equations above, TP and TN are the number of fibrosis and background pixels that were correctly identified. FP is the number of background pixels that are falsely identified as fibrosis, and FN is the number of fibrotic pixels that are detected as background. Hausdorff distance is an parameter which measures the maximum local distance between the predicted labels (A) and ground truth labels (B).

$$HD(A,B) = max_{b \epsilon B}\{min_{a \epsilon A}\{\sqrt{a^2 - b^2}\}\} \quad \text{(Eq. 6)}$$

Results

The table below shows the performance measures obtained by the model.

Table 1:Comparing the performance measures obtained by the model

Criteria	LV fibrosis	LV myocardium
Dice coefficient	89.74 ± 4.21	88.42 ± 1.18
Hausdorff distance	15.12 ± 6.53	17.34 ± 2.62
accuracy	98.22 ± 2.87	94.66 ± 66.3
precision	90.42 ± 3.24	89.84 ± 1.48
recall	88.47 ± 5.52	87.49 ± 3.45

Figure 3 compares the contours produced by the model (orange) and contours in the gold standard images (yellow).

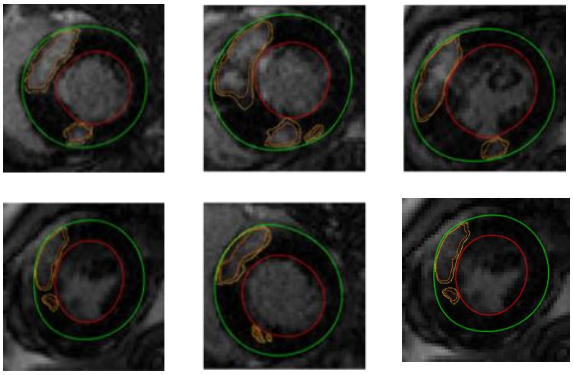

Figure 6: Comparing the results of the model with standard reference data

Discussion

We assessed the feasibility of using an Unet-based architecture to automate the process of fibrosis delineation in LGE images of HCM patients. This study aimed to reduce the time and expertise needed in the process of fibrosis assessment in HCM patients and achieved an accuracy of 98.22 and 94.66 in the delineation of fibrosis and LV myocardium, respectively. Compared to former works, this study obviates the need for pre-segmentations such as contouring myocardial borders and selecting initial seeds. There was also no need to use cine images in the training process. The necessity of contouring the myocardial borders, an essential prerequisite in most of the former works, is also eliminated.Compared to methods based on image intensity, not being vulnerable to the noise of images also helped to increase reproducibility and performance. This work is also one of the only studies focused on non-ischemic fibrosis like the one seen in HCM. The particular architecture and dilated convolutions used in that also help to achieve good performance without increasing the number of parameters. Due to some images' low contrast and noise, producing the gold standard images was challenging. The similarity between

myocardial borders and blood pools, along with and the low contrast and noise in some images made producing the gold standard images challenging. Therefore, using more standard ground truth images and broader datasets can help increase the model's reproducibility and accuracy.

References

1. Liew AC, Vassiliou VS, Cooper R, Raphael CE. Hypertrophic cardiomyopathy-past, present and future. J Clin Med. 2017;6(12):1-20.

2. Quarta G, Grasso A, Pasquale F, Flett AS, Sado DM, Bonini E, et al. Evolution and clinical importance of fibrosis in HCM. JACC Cardiovasc Imaging. 2011;4(11):1221–3.

3. Pagourelias ED, Alexandridis GM, Vassilikos VP. Fibrosis in hypertrophic cardiomyopathy: Role of novel echo techniques and multi-modality imaging assessment. Heart Fail Rev. 2021;26(6):1297–310.

4. Mewton N, Liu CY, Croisille P, Bluemke D, Lima JAC. Assessment of myocardial fibrosis with cardiovascular magnetic resonance. J Am Coll Cardiol. 2011;57(8):891-903.

5. Freitas P, Ferreira AM, Arteaga-Fernández E, De Oliveira Antunes M, Mesquita J, Abecasis J, et al. The amount of late gadolinium enhancement outperforms current guideline-recommended criteria in the identification of patients with hypertrophic cardiomyopathy at risk of sudden cardiac death. J Cardiovasc Magn Reson. 2019;21(1):1-10.

6. Greulich S, Seitz A, Herter D, Gunther F, Probst S, Bekeredjian R, et al. Long-term risk of sudden cardiac death in hypertrophic cardiomyopathy: A cardiac magnetic resonance outcome study. Eur Heart J Cardiovasc Imaging. 2021;22(7):732-41.

7. Neizel M, Katoh M, Schade E, Rassaf T, Krombach GA, Kelm M, et al. Rapid and accurate determination of relative infarct size in humans using contrast-enhanced magnetic resonance imaging. Clin Res Cardiol.2009 ;98(5):319–24.

8. Kolipaka A, Chatzimavroudis GP, White RD, O'Donnell TP, Setser RM. Segmentation of non-viable myocardium in delayed enhancement magnetic resonance images. Int J Cardiovasc Imaging. 2005;21(2-3):303-11.

9. Alba X, Figueras I Ventura RM, Lekadir K, Frangi AF. Healthy and scar myocardial tissue classification in DE-MRI. In: Camara O, Mansi T, Pop M, Rhode K, Sermesant M, Young A, editors. Proceedings of the Third International Workshop, STACOM 2012, Held in Conjunction with MICCAI 2012; 2012 Oct 5; Nice, France. Berlin, Germany: Springer; 2013. p. 62-70.

10. Lu Y, Connelly KA, Yang Y, Joshi SB, Wright G, Radau PE. Semi-automated analysis of infarct heterogeneity on DE-MRI using graph cuts. J Cardiovasc Magn Reson. 2012;14(1):1–3.

11. Ukwatta E, Arevalo H, Li K, Yuan J, Qiu W, Malamas P, et al. Myocardial infarct segmentation from magnetic resonance images for personalized modeling of cardiac electrophysiology. IEEE Trans Med Imaging. 2016;35(6):1408–19.

12. Ukwatta E, Yuan J, Qiu W, Wu KC, Trayanova N, Vadakkumpadan F. Myocardial infarct segmentation and reconstruction from 2D late-gadolinium enhanced magnetic resonance images. Med Image Comput Comput Assist Interv. 2014;17(02):554–61.

13. Usta F, Gueaieb W, White JA, Ukwatta E. 3D scar segmentation from LGE-MRI using a continuous max-flow method. Proceedings of the Medical Imaging 2018: Biomedical Applications in Molecular, Structural, and Functional Imaging; 2018 Feb 10-15; Houston, Texas, United States. Spie Medical Imaging; 2018.

14. Rajchl M, Yuan J, White JA, Ukwatta E, Stirrat J, Nambakhsh CMS, et al. Interactive hierarchical-flow segmentation of scar tissue from late-enhancement cardiac MR images. IEEE Trans Med Imaging. 2014;33(1):159–72.

15. Zabihollahy F, Rajchl M, White JA, Ukwatta E. Fully automated segmentation of left ventricular scar from 3D late gadolinium enhancement magnetic resonance imaging using a cascaded multi-planar U-Net (CMPU-Net). Med Phys. 2020;47(4):1645–55.

16. Kurzendorfer T, Breininger K, Steidl S, Brost A, Forman C, Maier A. Myocardial scar segmentation in LGE-MRI using fractal analysis and random forest classification. Proceedings of the 24th International Conference on Pattern Recognition (ICPR); 2018 Aug 20-24; Beijing, China. IEEE; 2018. p. 3168-73.

17. Larroza A, Materka A, Lopez-Lereu MP, Monmeneu JV, Bodi V, Moratal D. Differentiation between acute and chronic myocardial infarction by means of texture analysis of late gadolinium enhancement and cine cardiac magnetic resonance imaging. Eur J Radiol. 2017;92:78–83.

18. Zabihollahy F, White JA, Ukwatta E. Myocardial scar segmentation from magnetic resonance images using convolutional neural network. Proceedings of the Medical Imaging 2018: Computer-Aided Diagnosis; 2018 Feb 10-15; Houston, Texas, United States. Spie Medical Imaging; 2018.

19. Moccia S, Banali R, Martini C, Moscogiuri G, Pontone G, Pepi M, et al. Automated scar segmentation from CMR-LGE images using a deep learning approach. Proceedings of the Computing in Cardiology Conference (CinC); 2018 Sep 23-26; Maastricht, Netherlands. IEEE; 2019. p. 1-4.

20. Fahmy AS, Rausch J, Neisius U, Chan RH, Maron MS, Appelbaum E, et al. Automated cardiac MR scar quantification in hypertrophic cardiomyopathy using deep convolutional neural networks. JACC Cardiovasc Imaging. 2018;11(12):1917–8.

21. Popescu DM, Abramson HG, Yu R, Lai C, Shade JK, Wu KC, et al. Anatomically informed deep learning on contrast-enhanced cardiac magnetic resonance imaging for scar segmentation and clinical feature extraction. Cardiovasc Digit Health J. 2022;3(1):2–13.

22. Brahim K, Qayyum A, Lalande A, Boucher A, Sakly A, Meriaudeau F. A 3D network based shape prior for automatic myocardial disease segmentation in delayed-enhancement MRI. IRBM. 2021;42(6):424–34.

23. Heidenreich JF, Gassenmaier T, Ankenbrand MJ, Bley TA, Wech T. Self-configuring nnU-net pipeline enables fully automatic infarct segmentation in late enhancement MRI after myocardial infarction. Eur J Radiol. 2021;141:1-5.

24. Wang SH, McCann G, Tyukin I. Myocardial infarction detection and quantification based on a convolution neural network with online error correction capabilities. Proceedings of the International Joint Conference on Neural Networks (IJCNN); 2020 Jul 19-24; Glasgow, UK. IEEE; 2020. p. 1-8.

25. De la Rosa E, Sidibe D, Decourselle T, Leclercq T, Cochet A, Lalande A. Myocardial infarction quantification from late Gadolinium enhancement MRI using top-hat transforms and neural networks. Algorithms. 2021;14(8):1-18.

26. Fahmy AS, Rowin EJ, Chan RH, Manning WJ, Maron MS, Nezafat R. Improved quantification of myocardium scar in late Gadolinium enhancement images: Deep learning based image fusion approach. J Magn Reson Imaging. 2021;54(1):303–12.

27. Wang S, Singh VK, Cheah E, Wang X, Li Q, Chou SH, et al. Stacked dilated convolutions and asymmetric architecture for U-Net-based medical image segmentation. Comput Biol Med. 2022;148.